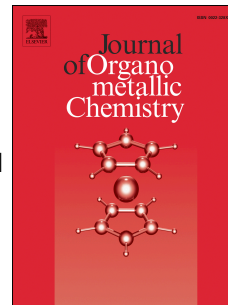


# Accepted Manuscript

Metallaheteroboranes containing group 16 elements: An experimental and theoretical study

Moulika Bhattacharyya, Rini Prakash, R. Jagan, Sundargopal Ghosh



PII: S0022-328X(19)30013-0

DOI: <https://doi.org/10.1016/j.jorganchem.2019.01.007>

Reference: JOM 20685

To appear in: *Journal of Organometallic Chemistry*

Received Date: 19 November 2018

Revised Date: 9 January 2019

Accepted Date: 11 January 2019

Please cite this article as: M. Bhattacharyya, R. Prakash, R. Jagan, S. Ghosh, Metallaheteroboranes containing group 16 elements: An experimental and theoretical study, *Journal of Organometallic Chemistry* (2019), doi: <https://doi.org/10.1016/j.jorganchem.2019.01.007>.

This is a PDF file of an unedited manuscript that has been accepted for publication. As a service to our customers we are providing this early version of the manuscript. The manuscript will undergo copyediting, typesetting, and review of the resulting proof before it is published in its final form. Please note that during the production process errors may be discovered which could affect the content, and all legal disclaimers that apply to the journal pertain.

## An experimental and theoretical study

Moulika Bhattacharyya, Rini Prakash, R. Jagan and Sundargopal Ghosh\*

Department of Chemistry, Indian Institute of Technology Madras, Chennai 600036, India

E-mail: [sghosh@iitm.ac.in](mailto:sghosh@iitm.ac.in), Fax: (+91) 44 2257 4202; Tel: (+91) 44 2257 4230

Keywords: oblatoarachno, metallaheteroboranes, tungsten, diphenyl dichalcogenide

### Abstract:

Thermolysis of diphenyl dichalcogenides,  $\text{Ph}_2\text{E}_2$  (E = S, Se and Te) with an insitu generated intermediate, obtained from the reaction of  $[\text{Cp}^*\text{WCl}_4]$  ( $\text{Cp}^* = \eta^5\text{-C}_5\text{Me}_5$ ) with  $[\text{LiBH}_4 \cdot \text{THF}]$ , yielded new tungstaheteroboranes,  $[(\text{Cp}^*\text{W})_2(\mu\text{-EPh})(\mu_3\text{-E})(\mu\text{-H})(\text{B}_3\text{H}_2\text{EPh})]$ , **1** and **2** (**1**: E = S; **2**: E = Se), and  $[(\text{Cp}^*\text{W})_2(\mu\text{-TePh})\text{B}_5\text{H}_5(\mu\text{-H})_3]$ , **4**. Formation of compounds **1** and **2** substantiate the evidence of  $[(\text{Cp}^*\text{W})_2\text{B}_4\text{H}_{10}]$ , which supports our previous studies. Compound **4** has a capped octahedral geometry that is unique due to the presence of three W-H-B bridging hydrogens in a *closo* cluster. Alternatively, the shape of cluster **4** can be defined as *oblatoarachno* that can be derived from a heptagonal bipyramid. All the compounds have been characterized by mass spectrometry,  $^1\text{H}$ ,  $^{11}\text{B}\{^1\text{H}\}$ , IR and  $^{13}\text{C}\{^1\text{H}\}$  NMR spectroscopy in solution and the structural architectures of **1** and **4** were unequivocally established by X-ray crystallographic analysis. The density functional theory calculations also yielded geometries in close agreement with the observed structures.

### 1. Introduction

Heteroborane chemistry is one of the robust branches of polyhedral borane chemistry, mainly due to the wide development of carboranes and their derivatives.<sup>1-3</sup> In parallel to the expansion of the carboranes, the chemistry of heteroboranes and heterometallaboranes containing group 16 elements have grown in numbers albeit in a slower rate, especially thiaboranes and thiametallaboranes.<sup>4-6</sup>

There is always an urge to synthesize the heavier chalcogen containing heterometallaborane and there has been a few success in this area.<sup>7-8</sup> From the earlier time, the strategies and reagents used for this purpose are varied and explored to make interesting cluster geometries.<sup>9-10</sup> Apart from this geometrical importance, many applications are also registered such as active homogeneous catalyst precursors in the hydrogenation and isomerization of alkenes.<sup>11-12</sup> Current investigations in our laboratory are focused on the development of new methods for the synthesis of dimetallaheteroboranes through the activation of diorganyl-dichalcogenide ligands<sup>13-14</sup> or chalcogen powders,<sup>15</sup> which have been shown to be one of the effective routes for the preparation of dimetallaheteroboranes.

In a recent study, we have described the direct evidence for the existence of saturated molybdaborane/tungstaborane compound,  $[(Cp^*M)_2B_4H_{10}]^{16}$  which was hypothesized earlier as  $[(Cp^*M)_2B_4H_8]^{17}$ . Therefore, there remains a possibility of similar analogues in metallaheteroboranes, which can substantiate this result further. Hence, in order to put some insight into this problem, we have reinvestigated the synthesis of group 6 heterometallaborane especially tungstaheteroborane where only a very few structurally characterized compounds are known.<sup>18</sup> The reaction led to the isolation of  $[(Cp^*W)_2(\mu-EPh)(\mu_3-E)(\mu-H)(B_3H_2EPh)]$  (E= S and Se) which supports the existence of a saturated tungstaborane compound  $[(Cp^*W)_2B_4H_{10}]$  as the intermediate. After perceiving success with S and Se, an investigation to isolate the Te analogues led to the formation of an unexpected  $[(Cp^*W)_2(\mu-TePh)B_5H_5(\mu-H)_3]$ , a new entry into the rare class of *oblatoarachno* geometry containing a bridging TePh ligand. Along with the other tools, density functional theory (DFT) calculations have been used to provide some insight into the nature of the bonding of these new molecules.

## 2. Results and discussion

### 2.1. Synthesis and characterizations of ditungstaheteroboranes, 1-4

As shown in Scheme 1, treatment of an insitu generated intermediate obtained from the reaction of  $Cp^*WCl_4$  with  $[LiBH_4 \cdot THF]$  at  $-78^\circ C$ , with  $Ph_2E_2$  [E= S, Se and Te] at  $85^\circ C$  led to the

isolation of tungstaheteroborane clusters  $[(Cp^*W)_2(\mu-EPh)(\mu_3-E)(\mu-H)(B_3H_2EPh)]$ , **1** and **2** (**1**: E = S; **2**: E = Se) and  $[(Cp^*W)_2(\mu-TePh)B_5H_5(\mu-H)_3]$ , **4** along with known  $[(Cp^*W)_2B_5H_9]$ , **3**.<sup>19</sup> Detailed characterizations of these molecules are described below.

(Scheme 1 near here)

### 2.1.1. $[(Cp^*W)_2(\mu-EPh)(\mu_3-E)(\mu-H)(B_3H_2EPh)]$ , **1** and **2** (**1**: E=S; **2**: E=Se):

Compound **1** was isolated as brown sticky semi solid in low yield. The mass spectral analysis of **1** shows the molecular ion peak at  $m/z$  924.1886 corresponding to  $[M]^+$ . The formation of new boron-containing species, **1** was indicated by the presence of three  $^{11}B\{^1H\}$  signals in 1:1:1 ratio at  $\delta = 91.8, 73.3$  and  $-12.2$  ppm indicating the presence of different boron environments. The  $^{11}B$  chemical shift at  $\delta = -12.2$  ppm can be assigned to the boron attached with the chalcogen atom which is a part of the cluster core. The  $^1H$  and  $^{13}C\{^1H\}$  NMR spectra imply two equivalents of  $Cp^*$  ligands. Further analysis of  $^1H$  NMR spectrum shows the presence of a single W-H-B proton at  $\delta = -7.81$  ppm. The characteristics bands for B-H<sub>t</sub> proton stretching frequency is observed at  $2498\text{ cm}^{-1}$ . These spectroscopic data were not adequate to envisage the identity of **1**. A clear explanation eluded us until the solid-state X-ray structure analysis of **1** was carried out.

(Fig. 1 near here)

The solid-state X-ray structure of **1**, shown in Fig. 1, is fully consistent with the spectroscopic data. The molecular structure of **1** consists of a planar unit of one sulphur and three boron atoms perpendicular to the W1-W2 bond and nearly parallel to the two  $Cp^*$  planes. In another way, the core structure can be considered as a bicapped tetrahedron similar to  $[(Cp^*ReH_2)_2B_4H_4]^{20}$  proposed by Fehlner *et al.* In compound **1**, two  $\{W_2B\}$  triangular faces are capped by one boron (B3) and sulphur (S3) atom in a  $\{W_2B_2\}$  tetrahedron and the W-W edge is further bridged by a sulfido ligand (S1), which led to a short W-W bond of  $2.6930(3)\text{ \AA}$  as compared to usual W-W single bond.<sup>19</sup> It is in between the double and single bond distance and very much comparable to that of  $[(Cp^*W)_2(\mu-S)_2(\mu-\eta^2-S_2CH_2)]$ .<sup>18c</sup> The shape of **1** can also be visualized as an *oblatoarachno* with the removal of

two equatorial vertices from *oblatocloso* hexagonal bipyramid with  $2n$  (12 e) Wadean<sup>21</sup> skeletal electrons (6 skeletal electron pairs). One of the interesting features of **1** is the presence of three different types of S- ligands, i)  $\mu_3$ - S, ii)  $\mu_2$ -SPh, iii) SPh. The  $\mu_3$ -S ligand is connected to the boron atom and the observed B(1)-S(3) bond length of 1.845(6) Å is comparable to that of other sulphur containing metalla-thiaborane compounds.<sup>7-8</sup> The  $\mu_2$ -SPh ligand bridge between two tungsten centres symmetrically with an average metal-sulfur bond length of 2.493 Å. This is comparable to the symmetric coordination of the disulfide bridges in  $[(Cp^*W)_2(\mu-S)_2(\mu-\eta^2-S_2CH_2)]$ .<sup>18c</sup>

As listed in Table 1, there are many *iso*-structural metallaboranes and metallaheteroboranes known to that of **1**, where a planar opened ring connected with two linear metal centers. One of the earlier examples is unsaturated chromaborane,  $[(Cp^*Cr)_2B_4H_8]$ .<sup>22</sup> Later various metallaboranes were synthesized and structurally characterized such as  $[(Cp^*Ta)_2B_4H_{10}]$ ,<sup>23a</sup>  $[(Cp^*ReH_2)_2B_4H_4]$ <sup>20</sup> with the same structure but different sep (skeletal electron pair) count. Other than the pure metallaboranes, a series of group 9 heterometallaboranes,  $[(Cp^*M)_2B_2E_2H_2]$ <sup>24-25</sup> (M= Co, Rh, Ir; E = S, Se) are also reported with the similar core. The analogues structurally characterized tungsten and molybdaborane compounds shown in Table 1 (entries 4-9) are *iso*-structural and *iso*-electronic to **1**. Compound **1** indeed is a mediator in the transition between  $[(Cp^*WCO)_2B_4H_6]$ , from which one and two boron atoms are replaced by sulphur atoms to form **1** and  $[(Cp^*W)_2(\mu-S)(\mu-\eta^4:\eta^4-S_2B_2H_2)]$  respectively. Even though there is not much deviation in the distance between two boron atoms (B1 and B2) in the  $M_2B_2$  tetrahedron core of bicapped tetrahedral geometry, the M-M bond distance is considerably shortened in case of chalcogen substituted complexes, mostly when bridging chalcogen present across the M-M bond. All the molybdenum and tungsten complexes, shown in Table 1, demonstrate the direct evidence for the formation of saturated molybda and tungstaborane compounds *i.e*  $[(Cp^*M)_2B_4H_{10}]$  (6 sep) as one of the possible intermediates.

(Table 1 near here)

In an attempt to extend this chemistry to heavier group-16 elements under similar reaction conditions, we have carried out the reaction of tungsten intermediate with Ph<sub>2</sub>Se<sub>2</sub> that led us to isolate the Se analogue of **1**, that is [(Cp\*W)<sub>2</sub>(μ-SePh)(μ<sub>3</sub>-Se)(μ-H)(B<sub>3</sub>H<sub>2</sub>SePh)], **2**. Several attempts to grow X-ray quality crystals of **2** were not achieved, however complete characterization of **2** was done based on the spectroscopic data. Compound **2** shows three resonances at δ = 108.3, 77.2 and 1.3 ppm in 1:1:1 ratio in <sup>11</sup>B{<sup>1</sup>H} NMR, whereas <sup>1</sup>H NMR shows presence of two equivalents of Cp\* ligand and one equivalent of bridging W-H-B proton. The mass spectrometry of compound **2** shows a molecular ion peak at *m/z* 1106.9778 corresponds to the molecular formula of C<sub>32</sub>H<sub>43</sub>B<sub>3</sub>KSe<sub>3</sub>W<sub>2</sub>.

Theoretical calculations on molecule **1'** (Cp analogue of **1**) reveal a satisfactory agreement between the density functional theory optimized and crystallographic structure (Table S1). The <sup>11</sup>B chemical shifts of **1'** and **2'**, calculated using the gauge including atomic orbital (GIAO) and B3LYP functional, agreed well with the experimental chemical shifts, listed in Table S2, hence confirming the structural assignments. Calculated natural charges (from natural bond orbital analysis (NBO), Table S4) complemented well with the <sup>11</sup>B chemical shifts which indeed show three dissimilar boron environments. The highest occupied molecular orbital (HOMO) and the lowest unoccupied molecular orbital (LUMO) energies as well as the HOMO–LUMO gap for the clusters **1'** and **2'** are listed in Supporting Information, Table S3. The computed substantial HOMO-LUMO gap of **1'** is around 3.25 eV, while it has reduced slightly in case of **2'** to 3.20 eV, that indicates the viability of these clusters. The HOMO-LUMO gap for **1'** and **2'** is in between [(Cp\*WCO)<sub>2</sub>B<sub>4</sub>H<sub>6</sub>]<sup>16</sup> (1.99 eV) and [(Cp\*W)<sub>2</sub>(μ-S)(μ-η<sup>4</sup>:η<sup>4</sup>-S<sub>2</sub>B<sub>2</sub>H<sub>2</sub>)]<sup>18c</sup> (3.50 eV) that indicates the increased stability upon the replacement of boron by chalcogen atom. The HOMO for both **1'** and **2'** is predominantly localized on metals and metal-boron bonds, whereas LUMO orbitals are oriented on metals and boron-boron bonds.

The nature of W-W bonding has been evaluated by the DFT calculations. The Wiberg bond index of 0.77 and 0.76 indicates a strong M-M interaction in **1'** and **2'** respectively. Following the same trend as HOMO-LUMO energy gap, the WBI values of M-M bond also increased from (Cp\*WCO)<sub>2</sub>B<sub>4</sub>H<sub>6</sub> (0.52) <**1'** <**2'** < (Cp\*W)<sub>2</sub>(μ-S)(μ-η<sup>4</sup>:η<sup>4</sup>-S<sub>2</sub>B<sub>2</sub>H<sub>2</sub>) (0.97) indicating the strengthening of cross cluster M-M bonding. The NBO (natural bond orbital) analysis shows the localized molecular orbital corresponding to M-M bond by the overlap of d<sub>z</sub><sup>2</sup> orbitals to form a σ-bond (Fig. 2(a)). Further, a strong σ bonding interaction has been observed between B1-S3 (WBI = 0.93) and B1-Se3 (WBI = 0.89) (Fig. S14(b) and Fig. S15(c)). There was no orbital overlap between the boron atoms, instead a 3c-2e bond between B1-B2-W2 in **1'** (Fig. S14(a)) and two 3c-2e bonds between B1-B2-W2 bond and B2-B3-W2 observed for **2'** (Fig. S15(a) and (b)). The nature of S-B, B-B and M-M interactions are also probed by QTAIM analysis. Fig.2(b) and (c) show the contour map of the Laplacian electron density Δ<sup>2</sup>ρ(r) along the S3-B1-B2-B3 plane of **1'** and Se3-B1-B2-B3 plane in **2'**. There is a strong bonding interaction present among the atoms in the corresponding plane in **2'**, whereas there is a slight charge depletion between B2-B3 in the plane of **1'** which can be attributed to the positive natural valence population of B3 (Table S4).

(Fig. 2 near here)

### 2.1.2. [(Cp\*W)<sub>2</sub>(μ-TePh)B<sub>5</sub>H<sub>5</sub>(μ-H)<sub>3</sub>], **4**

In an effort to synthesize the Te analogue of **1-2**, we have carried out the reaction of [Cp\*WCl<sub>4</sub>] with [LiBH<sub>4</sub>.THF] at -78°C followed by thermolysis with Ph<sub>2</sub>Te<sub>2</sub>. In contrast, extension of this approach to the diphenyl ditelluride resulted in the formation of [(Cp\*W)<sub>2</sub>(μ-TePh)B<sub>5</sub>H<sub>5</sub>(μ-H)<sub>3</sub>], **4**. Compound **4** has been isolated by thin layer chromatography (TLC) in low yield and the composition of **4** was recognized from the mass spectral analysis together with multinuclear NMR spectroscopy. The mass spectrum of the compound showed single molecular ion peak corresponding to C<sub>26</sub>H<sub>43</sub>B<sub>5</sub>TeW<sub>2</sub>Na, which is consistent with the formula containing five B, two W, and one Te atoms. The <sup>11</sup>B{<sup>1</sup>H} NMR spectrum shows four distinct boron environments appeared at δ = 64.9,

52.7, 9.4, and -14.1 ppm. The  $^1\text{H}$  NMR spectrum of **4** suggests the presence of single Cp\* resonance at  $\delta = 2.04$  ppm. In addition, the  $^1\text{H}$  spectrum reveals the presence of two kinds of W-H-B protons.

(Fig. 3 near here)

In order to confirm the spectroscopic assignments and to determine the solid state X-ray structure of **4**, the X-ray structure analysis was undertaken. Single crystals suitable for X-ray diffraction analysis of **4** were obtained from a mixture of hexane/ $\text{CH}_2\text{Cl}_2$  solution at  $-4^\circ\text{C}$ , thus allowing the structural characterization of  $[(\text{Cp}^*\text{W})_2(\mu\text{-TePh})\text{B}_5\text{H}_5(\mu\text{-H})_3]$  and confirm the structural inferences made on the basis of spectroscopic results. As shown in Fig.3(b), the structure of **4** can be described as a capped octahedron in which  $\{\text{W}_2\text{B}_4\}$  occupies the core vertices and capped by one  $\text{BH}_3$  unit over the  $\text{M}_2\text{B}$  face, similar to the geometry found in  $[(\text{Cp}^*\text{M})_3\text{B}_4\text{H}_4]^{26}$  ( $\text{M} = \text{Co}, \text{Rh}$  and  $\text{Ir}$ ). One of the interesting features of **4** is the presence of three bridging hydrogens, which cannot be seen in other *pileo*-capped octahedrons. The terminal hydrogen at the capping boron atom (B5) could not be located by X-Ray crystallography, however it has been confirmed by  $^1\text{H}$  NMR. In addition, the crystal structure of **4** does not display the W-H-B hydrogens, the position of the bridging W-H-B hydrides are assigned by comparing with those of the bicapped octahedron,  $[(\text{Cp}^*\text{W})_2\text{B}_6\text{H}_{10}]^{27}$ . The bridging hydrogens at  $\delta = -7.37$  and  $-12.97$  ppm of intensity ratio 1:2 are assigned to B1 and B5 borons respectively. The bridging hydrogen at  $\delta = -7.37$  ppm might be fluxional between W1 and W2, that makes both the metal centres symmetric. Hence, it displays single resonance for Cp\* and four resonances for boron in which the peak at  $\delta = 64.9$  ppm corresponds to equivalent B2 and B3 borons. Interestingly, the core geometry of **4** is first of its kind with  $\text{M}_2\text{B}_5$  unit, different from the earlier reported geometries, which are i) *oblatonido* geometry derived from the one vertex removal of hexagonal bipyramid observed in the case of  $[(\text{Cp}^*\text{Ta})_2\text{B}_5\text{H}_{11}]^{23a}$ ,  $[(\text{Cp}^*\text{M})_2\text{B}_5\text{H}_9]^{28}$  ( $\text{M} = \text{Mo}$  and  $\text{W}$ ) and  $[(\text{Cp}^*\text{ReH})_2\text{B}_5\text{Cl}_5]^{29}$  ii) *oblatoarachno* structure with the example of  $[\{(\eta^5\text{-C}_5\text{Me}_5)\text{TaCl}\}_2\text{B}_5\text{H}_{11}]^{23b}$ .

The W-W bond length of 2.848 Å in **4** is somewhat shorter as compared to  $[(Cp^*W)_2B_6H_{10}]^{27}$  but longer than  $[(Cp^*W)_2B_5H_9]^{28}$  and **1**. The W-B bond lengths have shown variation within the cluster. The hydrogen-bridged linkages are of comparable length to those found in  $[(Cp^*W)_2B_5H_9]$  (average 2.24 Å). Likewise, the W-B bond, B-B distances are also of different ranges from 1.63-1.85 Å, among which the shortest bond is found between B2-B3 and longest between B4-B5 atoms. On the other hand, the  $\mu$ -Te ligands which is bridged between two tungsten centres are symmetric with an average bond length of 2.711 Å.

(Fig. 4 near here)

On the basis of capping principle that predicts capped-*closo* geometry for *n*-vertex polyhedra having *n* skeletal electron pairs is validated in case of **4** with 7 sep. Although the observed capped octahedral *closo*-cluster geometry is well documented, such clusters with three edge-bridging W-H-B hydrogens are rare. Hence in a close inspection, we found that it is slightly distorted than normal capped octahedron which make one of its face open to some extent. So, in an alternative way the geometry of **4** can be explained as *oblatoarachno* geometry derived from heptagonal bipyramid with two diamond-square-diamond (DSD) rearrangements and removal of two vertices (Fig. 4). The electron count satisfies with this finding by having *oblatoarachno* polyhedron with *n* vertices have  $(2(n+2)-4) = 2n$  (14 e or 7 ep) Wadean skeletal electrons.<sup>30</sup> The core reported for  $[(\eta^5-C_5Me_5)TaCl]_2B_5H_{11}]^{23b}$  is a structural isomer of the geometry reported for **4**. The electron count for **4** can also be validated using Mingos's fusion formalism. According to Mingos's approach, condensation process occurs by vertex, edge or face sharing.<sup>31</sup> The total electron count in such condensed clusters is equal to the sum of the electron count of the parent polyhedra minus the electron count of the shared units (atom, pair of atoms etc.). The total cluster valence electrons (cve) available for **4** is 48 [ $2Cp^*W$  ( $2 \times 11 = 22$ ) +  $5B$  ( $5 \times 3 = 15$ ) +  $8H$  ( $8 \times 1 = 8$ ) +  $\mu$ -TePh (3) = 48]. The geometry of **4** can be considered as a fused cluster in which an octahedron and a tetrahedron cluster got fused via a triangular  $W_2B$  face. Thus, if one applies Mingos's fusion formalism for this cluster,

this would give 48 electrons (octahedron [W<sub>2</sub>B<sub>4</sub>] (46 e) + tetrahedron [W<sub>2</sub>B<sub>2</sub>] (40 e) - triangle [W<sub>2</sub>B] (38 e) = 48 e).

Quantum chemical calculations at the B3LYP/6-31G\* level for the structure of **4'** (Cp analogue of **4**) yielded optimized geometries in good agreement with the crystallographically determined structure (Table S1). Likewise, the GIAO calculated chemical shifts and resonance assignments are listed in Table S2, which are in accord with the experimental values obtained from the NMR studies. The molecular orbital analysis shows the HOMO-LUMO gap of 2.25 eV that indicates its high stability. The WBI values of 0.64 further supports a strong M-M bond which is slightly weaker than **1'**. A very strong bonding interaction has also been found between W-Te (WBI = 0.83 and 0.87). Natural bond order analysis shows the bonding orbitals between W-W with the occupancy of 1.71 by the overlap of d<sub>z</sub><sup>2</sup> orbitals (Fig S16). Interestingly there is a 3c-2e bond present between B1-B2-B3 and B4-B3-B2 (Fig. 5). The topology analysis shows a high charge concentrated area around B1-B2-B3 plane forming a triangular ring (Fig. 5(b)). The strong covalent character of boron-boron bond is indicated by higher values of electron density ( $\rho(r)$ ) and a negative value of energy density (H(r)) at bond critical point (bcp) (Table S5). Natural charge and valence population analysis shows a high electron donating nature of Te atom (Table S4).

(Fig. 5 near here)

### 3. Conclusion

The results described herein demonstrate the synthesis and structural characterization of a series of di-tungstaheteroborane molecules. Compounds **1** and **2** are the derivatives of *nido*-[(Cp\*M)<sub>2</sub>B<sub>4</sub>H<sub>10</sub>], in which one of the vertices is substituted by S and Se respectively. We have also isolated and structurally characterized one ditungstaheteroborane cluster **4** with capped octahedron geometry. Although the structural type of **4** is well known, the presence of three W-H-B bridging hydrogens is

exceptional for a *closo* cluster. The experimental results have also been complemented and rationalized by means of DFT studies.

## 4. Experimental details

### 4.1. General procedures and instrumentation

All the syntheses were carried out under argon atmosphere with standard Schlenk and glove box techniques. Solvents were dried by common methods and distilled under N<sub>2</sub> before use. [Cp\*WCl<sub>4</sub>]<sup>32</sup> were prepared according to literature method while other chemicals, LiBH<sub>4</sub>·THF and Ph<sub>2</sub>E<sub>2</sub> (E=S, Se, Te) are purchased from Aldrich chemicals and used as received. The external reference for the <sup>11</sup>B NMR, [Bu<sub>4</sub>N(B<sub>3</sub>H<sub>8</sub>)] was synthesized according to literature method.<sup>33</sup> Thin layer chromatography was carried on 250-mm diameter aluminium supported silica gel TLC plates (MERCK TLC Plates). NMR spectra were recorded on 400 and 500 MHz Bruker FT-NMR spectrometers. The residual solvent protons were used as reference ( $\delta$ , ppm, d<sub>6</sub>-benzene, 7.16, CDCl<sub>3</sub>, 7.26), while a sealed tube containing [Bu<sub>4</sub>N(B<sub>3</sub>H<sub>8</sub>)] in d<sub>6</sub>-benzene ( $\delta$ <sub>B</sub>, ppm, -30.07) was used as an external reference for the <sup>11</sup>B NMR. Mass spectra were recorded with a Bruker MicroTOF-II mass spectrometer in ESI ionization mode. Infrared spectra were recorded with a JASCO FT/IR-4100 spectrometer. Due to low yields, oily nature and higher sensitivity of these compounds, the elemental as well as melting point analysis could not be carried out. Thus, the combustion analysis and melting point data are not reported.

### 4.2. Synthesis of 1-4

In a Flame-dried Schlenk tube, [Cp\*WCl<sub>4</sub>], (0.5 g, 1.08 mmol) was suspended in toluene (20 mL) and cooled to -78<sup>0</sup>C. LiBH<sub>4</sub>·THF (2.16 mL, 4.32 mmol) was added via syringe, and the reaction mixture was warmed slowly over 20 min to room temperature and left stirring for an additional hour. The solvent was evaporated under vacuum, and the residue extracted into hexane. The brownish green hexane extract was thermolyzed at 85<sup>0</sup>C with excess of diphenyl disulfide, PhS-SPh (0.9 g, 4.32 mmol) for 18h. The solvent was removed in vacuo, and the residue was extracted into hexane.

After removal of solvent from the filtrate, the residue was subjected to chromatographic work up using silica gel TLC plates. Elution with hexane/CH<sub>2</sub>Cl<sub>2</sub> (95:05 v/v) yielded brown oily solid [(Cp\*W)<sub>2</sub>(μ-SPh)(μ<sub>3</sub>-S)(μ-H)(B<sub>3</sub>H<sub>2</sub>SPh)], **1** (0.06 g, 6%). Under the similar reaction conditions, diphenyl diselenide, PhSe-SePh (1.34 g, 4.32 mmol) yielded brown oily solid [(Cp\*W)<sub>2</sub>(μ-SePh)(μ<sub>3</sub>-Se)(μ-H)(B<sub>3</sub>H<sub>2</sub>SePh)], **2** (0.04 g, 3%), whereas diphenyl ditelluride, Ph<sub>2</sub>Te<sub>2</sub> (1.76 g, 4.32 mmol) produced [(Cp\*W)<sub>2</sub>(μ-TePh)B<sub>5</sub>H<sub>5</sub>(μ-H)<sub>3</sub>], **4** (0.05 g, 5%), as a red oily solid.

Note that compounds **1**, **2** and **4** have been isolated along with the yellow solid metallaborane, [(Cp\*W)<sub>2</sub>B<sub>5</sub>H<sub>9</sub>],<sup>19</sup> **3**, in ~10-12% yield.

**1**: MS (ESI<sup>+</sup>): *m/z* calcd for C<sub>32</sub>H<sub>43</sub>B<sub>3</sub>S<sub>3</sub>W<sub>2</sub><sup>+</sup>: 924.1825 [M]<sup>+</sup>, found: 924.1886 [M]<sup>+</sup>; <sup>11</sup>B{<sup>1</sup>H} NMR (160 MHz, CDCl<sub>3</sub>, 22 °C): δ = 91.8 (s, 1B), 73.3 (s, 1B), -12.2 (s, 1B) ppm; <sup>1</sup>H NMR (500 MHz, CDCl<sub>3</sub>, 22 °C): δ = 7.52 - 6.99 (m, C<sub>6</sub>H<sub>5</sub>), 8.63 (pcq, 1H, BH<sub>i</sub>), -2.06 (br, 1B-H<sub>i</sub>), 2.28 (s, 15H, Cp\*) 1.83 (s, 15H, Cp\*), -7.81 (s, 1H, M-H-B) ppm; <sup>13</sup>C{<sup>1</sup>H} NMR (125 MHz, CDCl<sub>3</sub>, 22 °C): δ = 134.03- 127.33 (s, C<sub>6</sub>H<sub>5</sub>), 104.76 (s, C<sub>5</sub>Me<sub>5</sub>), 104.51 (s, C<sub>5</sub>Me<sub>5</sub>), 12.80 (s, C<sub>5</sub>Me<sub>5</sub>), 12.46 (s, C<sub>5</sub>Me<sub>5</sub>); IR (hexane, cm<sup>-1</sup>): 2498w (BH<sub>i</sub>).

**2**: HRMS (ESI<sup>+</sup>): *m/z* calcd for C<sub>32</sub>H<sub>43</sub>B<sub>3</sub>KS<sub>2</sub>W<sub>2</sub><sup>+</sup>: 1106.9796 [M+K]<sup>+</sup>, found: 1106.9778 [M+K]<sup>+</sup>; <sup>11</sup>B{<sup>1</sup>H} NMR (160 MHz, CDCl<sub>3</sub>, 22 °C): δ = 108.3 (s, 1B), 77.2 (s, 1B), 1.3 (s, 1B) ppm; <sup>1</sup>H NMR (500 MHz, CDCl<sub>3</sub>, 22 °C): δ = 7.52 - 7.05 (m, C<sub>6</sub>H<sub>5</sub>), 9.28 (pcq, 1H, BH<sub>i</sub>), -0.73 (br, 1B-H<sub>i</sub>), 2.19 (s, 15H, Cp\*), 2.13 (s, 15H, Cp\*), -8.72 (s, 1H, M-H-B) ppm; <sup>13</sup>C{<sup>1</sup>H} NMR (125 MHz, CDCl<sub>3</sub>, 22 °C): δ = 133.43- 127.57 (s, C<sub>6</sub>H<sub>5</sub>), 104.38 (s, C<sub>5</sub>Me<sub>5</sub>), 104.23 (s, C<sub>5</sub>Me<sub>5</sub>), 13.28 (s, C<sub>5</sub>Me<sub>5</sub>), 12.95 (s, C<sub>5</sub>Me<sub>5</sub>); IR (hexane, cm<sup>-1</sup>): 2495w (BH<sub>i</sub>).

**4**: HRMS (ESI<sup>+</sup>): *m/z* calcd for C<sub>26</sub>H<sub>43</sub>B<sub>5</sub>NaTeW<sub>2</sub><sup>+</sup>: 931.1809 [M+Na]<sup>+</sup>, found: 931.1825 [M+Na]<sup>+</sup>; <sup>11</sup>B{<sup>1</sup>H} NMR (160 MHz, CDCl<sub>3</sub>, 22 °C): δ = 64.9 (s, 2B), 52.7 (s, 1B), 9.4 (s, 1B), -14.1(s, 1B) ppm; <sup>1</sup>H NMR (500 MHz, CDCl<sub>3</sub>, 22 °C): δ = 7.40 -7.10 (m, C<sub>6</sub>H<sub>5</sub>), 8.46 (br, 1H, B-H<sub>i</sub>), 8.07 (br, 1H, B-H<sub>i</sub>), 4.42(br, 2H, B-H<sub>i</sub>), -0.90 (pcq, 1H, B-H<sub>i</sub>), 2.04 (s, 30H, Cp\*), -7.37 (s, 1H, M-H-B), -

12.97 (s, 2H, M-H-B) ppm;  $^{13}\text{C}\{^1\text{H}\}$  NMR (125 MHz,  $\text{CDCl}_3$ , 22 °C):  $\delta$  = 130.06 - 127.58 (s,  $\text{C}_6\text{H}_5$ ), 100.85 (s,  $\text{C}_5\text{Me}_5$ ), 13.00 (s,  $\text{C}_5\text{Me}_5$ ); IR (hexane,  $\text{cm}^{-1}$ ): 2412w, 2502w (B-H<sub>1</sub>).

#### 4.3. Computational details.

The Quantum chemical calculations were performed on the simplified model compounds **1'**, **2'**, and **4'** (Cp analogues of **1**, **2**, and **4**) using the Gaussian 09 program package.<sup>34</sup> Geometry optimization were conducted in the gaseous state (no solvent effect) without any symmetry constraints using the BP86<sup>35</sup> functional paired with a mixed basis set: Stuttgart/Dresden double- $\zeta$ (SDD) effective core potentials (ECPs)<sup>36</sup> for W; 6-31g\* basis set for the other atoms. The optimized geometries were characterized as true minima by using analytical frequency calculations. The gauge including atomic orbital (GIAO)<sup>37</sup> method has been employed to compute the NMR chemical shifts with hybrid Becke-Lee-Yang-Parr (B3LYP) functional<sup>38</sup> with the BP86/6-31g\*, SDD optimized geometries. The  $^{11}\text{B}$  NMR chemical shifts were calculated relative to  $\text{B}_2\text{H}_6$  (B3LYP/6-31g\* B shielding constant, 93.5 ppm) and converted to the usual  $[\text{BF}_3\cdot\text{OEt}_2]$  scale by using the experimental  $\delta(^{11}\text{B})$  value of  $\text{B}_2\text{H}_6$  ( $\delta$  = 16.6 ppm).<sup>39</sup> TMS ( $\text{SiMe}_4$ ) was used as the internal standard for the  $^1\text{H}$  NMR chemical shift calculations. The  $^1\text{H}$  chemical shifts were referenced to TMS. Wiberg bond indices (WBIs)<sup>40</sup> were obtained from a natural bond orbital (NBO)<sup>41</sup> analysis. All the optimized structures and orbital graphics were generated by using the Chemcraft.<sup>42</sup> The two dimensions of the electron density and the Laplacian electronic distribution plots were generated using the Multiwfn package.<sup>43</sup>

#### 4.4. X-ray crystal structure determinations

Crystallographic information for **1** and **4** are shown in Table 2. The crystal data for **1** and **4** were collected and integrated using a Bruker kappa apex2 CCD diffractometer, with graphite-monochromated  $\text{MoK}_\alpha$  ( $\lambda$  = 0.71073 Å) radiation at 273 K. The structures were solved by heavy atom methods using SHELXS-2016 and refined by using SHELXL-2016 (Sheldrick, G.M., University of Göttingen)<sup>44</sup>

(Table 2 near here)

The authors declare no competing financial interest.

### Acknowledgements

This project was supported by the Council of Scientific and Industrial Research (CSIR; No. 01(2837)/15/EMR-II), New Delhi, India. DST-FIST, India, is gratefully acknowledged for the HRMS facility. M.B and R. P are grateful to IIT Madras for fellowship. The computational facility of IIT Madras is gratefully acknowledged. We thank Mr. C. Ghosh for X-ray data collection.

### Appendix A. Supplementary data

Supplementary data related to this article can be found at <http://dx.doi.org>

### References

- (1) (a) R. N. Grimes, *Coord. Chem. Rev.* 200-202 (2000) 773-881;  
(b) R. N. Grimes, in E. W. Abel, G. Wilkinson, and F. G. A. Stone (Eds.), *Transition Metal Metallocarbaboranes*, pp 373-430, *Comprehensive Organometallic Chemistry II*, Vol 1, Pergamon, New York, 1995.
- (2) (a) M. F. Hawthorne, G. B. Dunks, *Science* 178 (1972) 462-471;  
(b) N. S. Hosmane, R. N. Grimes, *Inorg. Chem.* 18 (1979) 2886-2891;  
(c) A. K. Saxena, N. S. Hosmane, *Chem. Rev.* 93 (1993) 1081-1124.
- (3) (a) R. N. Grimes, *Carboranes*, Academic Press, Elsevier, Oxford, UK, 3rd edn, (2016);  
(b) R. E. Williams, *Inorg. Chem.* 10 (1971) 210-214;  
(c) R. N. Grimes, *Collect. Czech. Chem. Commun.* 67 (2002) 728-750.
- (4) (a) G. D. Friesen, A. Barriola, P. Daluga, P. Ragatz, J. C. Huffman, L. J. Todd, *Inorg. Chem.* 19 (1980) 458-462;  
(b) N. C. Norman, A. G. Orpen, M. J. Quayle, C. R. Rice, *New J. Chem.* 24 (2000) 837-839;

- (c) A. Hammerschmidt, M. Döch, S. Pütz, B. Krebs, *Z. Anorg. Allg. Chem.* 631 (2005) 1125-1329.
- (5) (a) B. Frange, J. D. Kennedy, *Main Group Met. Chem.* 19 (1996) 1775-1777;  
(b) G. Ferguson, J. D. Kennedy, X. L. R. Fontaine, Faridoon, T. R. Spalding, *J. Chem. Soc., Dalton Trans.* (1988) 2555-2564.  
(c) J. D. Kennedy, *Prog. Inorg. Chem.* 32 (1984) 519-679;  
(d) J. D. Kennedy, *Prog. Inorg. Chem.* 34 (1986) 211-434;
- (6) (a) G. Ferguson, J. F. Gallagher, J. D. Kennedy, A.-M. Kelleher, T. R. Spalding, *Dalton Trans.* (2006) 2133-2139;  
(b) S. K. Bose, S. M. Mobin, S. Ghosh, *J. Organomet. Chem.* 696 (2011) 3121-3126;  
(c) A. Thakur, S. Sao, V. Ramkumar, S. Ghosh, *Inorg. Chem.* 51 (2012) 8322-8330.
- (7) (a) R. S. Dhayal, K. K. V. Chakrahari, B. Varghese, S. M. Mobin, S. Ghosh, *Inorg. Chem.* 49 (2010) 7741-7747;  
(b) S. Sahoo, S. M. Mobin, S. Ghosh, *J. Organomet. Chem.* 695 (2010) 945-949.
- (8) (a) D. K. Roy, S. K. Bose, K. Geetharani, K. K. V. Chakrahari, S. M. Mobin, S. Ghosh, *Chem. Eur. J.* 18 (2012) 9983-9991;  
(b) B. Mondal, M. Bhattacharyya, B. Varghese S. Ghosh, *Dalton Trans.* 45 (2016) 10999-11007;  
(c) B. S. Krishnamoorthy, A. Thakur, K. K. V. Chakrahari, S. K. Bose, P. Hamon, T. Roisnel, S. Kahlal, S. Ghosh, J. -F. Halet, *Inorg. Chem.* 51 (2012) 10375-10383.
- (9) (a) B. Joseph, S. Gomosta, S. K. Barik, S. K. Sinha, T. Roisnel, V. Dorcet, J.-F. Halet, S. Ghosh, *J. Organomet. Chem.* 865 (2018) 29-36;  
(b) K. Geetharani, S. K. Bose, S. Ghosh, *Pure Appl. Chem.* 84 (2012) 2233-2241.
- (10) (a) S. K. Bose, K. Geetharani, S. Sahoo, K. H. K. Reddy, B. Varghese, E. D. Jemmis, S. Ghosh, *Inorg. Chem.* 50 (2011) 9414-9422;  
(b) C. E. Rao, K. Yuvaraj, S. Ghosh, *J. Organomet. Chem.* 776 (2015) 123-128;  
(c) S. K. Bose, K. Geetharani, V. Ramkumar, B. Varghese, S. Ghosh, *Inorg. Chem.* 49 (2010) 2881-2888.

- (11) À. Àlvarez, R. Macías, J. Bould, M. J. Fabra, F. J. Lahoz, L. A. Oro, *J. Am. Chem. Soc.* 130, (2008) 11455-11466;
- (12) D. E. Kadlecck, P. J. Carroll, L. G. Sneddon, *J. Am. Chem. Soc.* 122 (2000) 10868-10877.
- (13) S. K. Barik, M. G. Chowdhury, S. De, P. Parameswaran, S. Ghosh, *Eur. J. Inorg. Chem.* (2016) 4546-4550.
- (14) M. G. Chowdhury, S. K. Barik, K. Saha, K. Bakthavachalam, A. Banerjee, V. Ramkumar, S. Ghosh, *Inorg. Chem.* 57 (2018) 985-994.
- (15) S. Kar, K. Saha, S. Saha, K. Bakthavachalam, V. Dorcet, S. Ghosh, *Inorg. Chem.* 57 (2018) 10896-10905;
- (16) B. Mondal, R. Bag, S. Ghosh, *Organometallics* 37 (2018) 2419-2428.
- (17) S. Aldridge, M. Shang, T. P. Fehlner, *J. Am. Chem. Soc.* 120 (1998) 2586-2598.
- (18) (a) K. K. V. Chakrahari, A. Thakur, B. Mondal, V. Ramkumar, S. Ghosh, *Inorg. Chem.* 52 (2013) 7923-7932;
- (b) S. Sahoo, K. H. K. Reddy, R. S. Dhayal, S. M. Mobin, V. Ramkumar, E. D. Jemmis, S. Ghosh, *Inorg. Chem.* 48 (2009) 6509-6516;
- (c) B. Mondal, R. Bag, K. Bakthavachalam, B. Varghese, S. Ghosh, *Eur. J. Inorg. Chem.* (2017) 5434-5441.
- (19) A. S. Weller, M. Shang, T. P. Fehlner, *Organometallics* 18 (1999) 53-64.
- (20) S. Ghosh, M. Shang, T. P. Fehlner, *J. Organomet. Chem.* 614-615 (2000) 92-98.
- (21) (a) K. Wade, *Adv. Inorg. Chem. Radiochem.* 18 (1976) 1-66;
- (b) K. Wade, *Inorg. Nucl. Chem. Lett.* 8 (1972) 559-562.
- (22) K. J. Deck, Y. Nishihara, M. Shang, T. P. Fehlner, *J. Am. Chem. Soc.* 116 (1994) 8408-8409.

- (23) (a) S. K. Bose, K. Geetharani, B. Varghese, S. M. Mobin, S. Ghosh, *Chem. Eur. J.* 14 (2008) 9058-9064;
- (b) K. Geetharani, B. S. Krishnamoorthy, S. Kahlal, S. M. Mobin, J. -F. Halet, S. Ghosh, *Inorg. Chem.* 51 (2012) 10176-10184.
- (24) B. Joseph, S. K. Barik, R. Ramalakshmi, G Kundu, T. Roisnel, V. Dorcet, S. Ghosh, *Eur. J. Inorg. Chem.* (2018) 2045-2053.
- (25) (a) R. P. Micciche, P. J. Carroll, L. G. Sneddon, *Organometallics* 4 (1985) 1619-1623;
- (b) D. Sharmila, R. Ramalakshmi, K. K. V. Chakrahari, B. Varghese, S. Ghosh, *Dalton Trans.* 43 (2014) 9976-9985;
- (c) S. K. Barik, V. Dorcet, T. Roisnel, J. -F. Halet, S. Ghosh, *Dalton Trans.* 44 (2015) 14403-14410.
- (26) (a) T. L. Venable, E. Sinn, R. N. Grimes, *Inorg. Chem.* 21 (1982) 904-908;
- (b) H. Yan, A. M. Beatty, T. P. Fehlner, *Organometallics* 21 (2002) 5029-5037;
- (c) R. Borthakur, R. Prakash, P. Nandi, S. Ghosh, *J. Organomet. Chem.* 825–826 (2016) 1-7.
- (27) S. K. Bose, B. C. Noll, J. -F. Halet, J. Y. Saillard, A. Vega, S. Ghosh, *Organometallics* 26 (2007) 5377-5385.
- (28) (a) S. Aldridge, M. Shang, T. P. Fehlner, *J. Am. Chem. Soc.* 119 (1997) 2339-2340;
- (b) A. S. Weller, M. Shang, T. P. Fehlner, *Organometallics* 18 (1999) 53-64.
- (29) B. L. Guennic, H. Jiao, S. Kahlal, J. -Y. Saillard, J. -F. Halet, S. Ghosh, M. Shang, A. M. Beatty, A. L. Rheingold, T. P. Fehlner, *J. Am. Chem. Soc.* 126 (2004) 3203-3217.
- (30) R. B. King, *Inorg. Chem.* 45 (2006) 8211-8216.
- (31) (a) D. M. P. Mingos, *Nat. Phys. Sci.* 236 (1972) 99-102;
- (b) D. M. P. Mingos, *Acc. Chem. Res.* 17 (1984) 311-319;

Hall, New York, 1990.

(32) (a) M. L. H. Green, J. D. Hubert, P. Mountford, *J. Chem. Soc., Dalton Trans.* (1990) 3793-3800;

(b) M. Kaushika, A. Singh, M. Kumar, *Eur. J. Chem.* 3 (2012) 367-394.

(33) G. E. Ryschkewitsch, K. C. Nainan, *Inorg. Synth.* 15 (1974) 113-114.

(34) Gaussian 09, Revision C.01, M. J. Frisch, G. W. Trucks, H. B. Schlegel, G. E. Scuseria, M. A. Robb, J. R. Cheeseman, G. Scalmani, V. Barone, B. Mennucci, G. A. Petersson, H. Nakatsuji, M. Caricato, X. Li, H. P. Hratchian, A. F. Izmaylov, J. Bloino, G. Zheng, J. L. Sonnenberg, M. Hada, M. Ehara, K. Toyota, R. Fukuda, J. Hasegawa, M. Ishida, T. Nakajima, Y. Honda, O. Kitao, H. Nakai, T. Vreven, J. A. Montgomery, Jr. J. E. Peralta, F. Ogliaro, M. Bearpark, J. J. Heyd, E. Brothers, K. N. Kudin, V. N. Staroverov, T. Keith, R. Kobayashi, J. Normand, K. Raghavachari, A. Rendell, J. C. Burant, S. S. Iyengar, J. Tomasi, M. Cossi, N. Rega, J. M. , M. Klene, J. E. Knox, J. B. Cross, V. Bakken, C. Adamo, J. Jaramillo, R. Gomperts, R. E. Stratmann, O. Yazyev, A. J. Austin, R. Cammi, C. Pomelli, J. W. Ochterski, R. L. Martin, K. Morokuma, V. G. Zakrzewski, G. A. Voth, P. Salvador, J. J. Dannenberg, S. Dapprich, A. D. Daniels, O. Farkas, J. B. Foresman, J. V. Ortiz, J. Cioslowski, D. J. Fox, Gaussian Inc., Wallingford CT (2010).

(35) H. L. Schmider, A. D. Becke, *J. Chem. Phys.* 108 (1998) 9624-9631.

(36) M. Dolg, H. Stoll, H. Preuss, *Theor. Chim. Acta.* 85 (1993) 441-450.

(37) (a) F. J. London, *J. Phys. Radium* 8 (1937) 397-409;

(b) R. Ditchfield, *Mol. Phys.* 27 (1974) 789-807;

(c) K. Wolinski, J. F. Hinton, P. Pulay, *J. Am. Chem. Soc.* 112 (1990) 8251-8260.

(38) C. Lee, W. Yang, R. G. Parr, *Phys. Rev. B* 37 (1988) 785-789.

(39) T. P. Onak, H. L. Landesman, R. E. Williams, I. Shapiro, J. Phys. Chem. 63 (1959) 1533–1535.

(40) K. Wiberg, Tetrahedron 24 (1968) 1083-1096.

(41) (a) A. E. Reed, L. A. Curtiss, F. Weinhold, Chem. Rev. 88 (1988) 899-926;

(b) F. Weinhold, C. R. Landis, Valency and Bonding: A Natural Bond Orbital Donor-Acceptor Perspective, Cambridge University Press, Cambridge (2005);

(c) R. B. King, Inorg. Chem. 1999, 38, 5151-5153;

(d) R. B. King, Inorg. Chim. Acta. 300 (2000) 537-544.

(42) Chemcraft - graphical software for visualization of quantum chemistry computations.

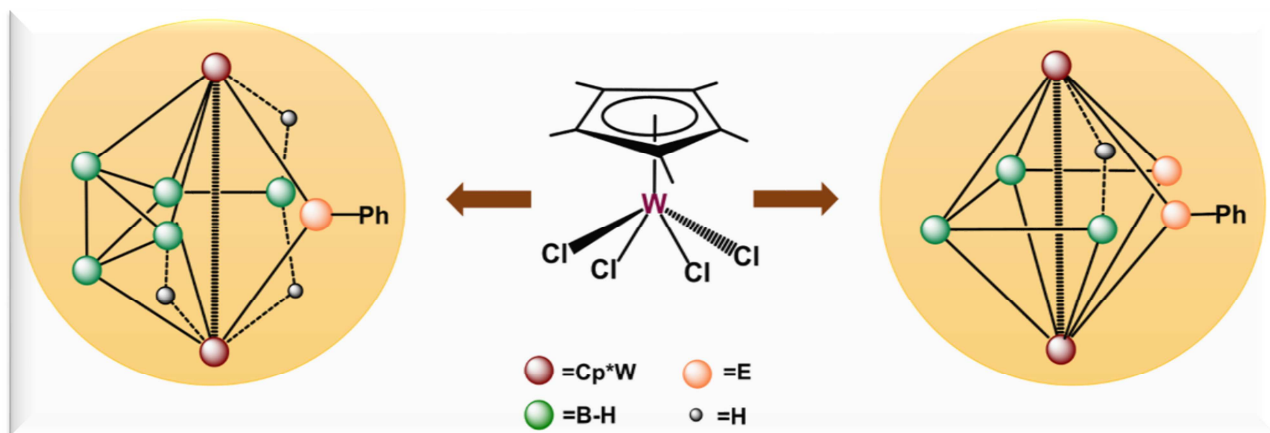
<https://www.chemcraftprog.com>.

(43) T. Lu, F. Chen, J. Comput. Chem. 33 (2012) 580-592.

(44) (a) G. M. Sheldrick, Acta Cryst. A 71 (2015) 3-8;

(b) G. M. Sheldrick, Acta Cryst. C 71 (2015) 3-8.

New tungstaheteroboranes,  $[(Cp^*W)_2(\mu-EPh)(\mu_3-E)(\mu-H)(B_3H_2EPh)]$ , an analogue of  $[(Cp^*W)_2B_4H_{10}]$  (right) and  $[(Cp^*W)_2(\mu-TePh)B_5H_5(\mu-H)_3]$ , a capped octahedron having three W-H-B bridging hydrogens (left).



**Scheme 1** Synthesis of dimetallaheteroborane clusters **1-4**

**Fig. 1** Molecular structure and labeling diagram of **1**. Selected bond lengths ( $\text{\AA}$ ) and bond angles ( $^\circ$ ): W1-W2 2.6930(3), B1-B2 1.691(9), B1-S3 1.845(6), B1-W2 2.332(7), B2-W1 2.244(6), S1-W1 2.5244(14), W2-S3 2.4119(16); B2-B1-S3 123.1(4), S3-B1-W1 69.3(2), W1-B1-W2 70.86(19), W2-S1-W1 65.36(3), B3-W1-W2 49.63(17), B1-S3-W2 64.9(2).

**Table 1** Skeletal electron pair (sep) count, structural parameters and chemical shift of  $M_2B_4$  core or its derivatives

**Fig. 2** (a)  $\sigma$  bonding orbital of W1-W2 from NBO analysis of **1'** (contour value:  $\pm 0.05$  [ $e/\text{bohr}^3$ ] $^{1/2}$ ), (b) and (c) showing the contour line diagrams of the Laplacian of the electron density,  $\nabla^2\rho(r)$  of S3-B1-B2-B3 plane in **1'** and Se3-B1-B2-B3 plane in **2'** that generated using the Multiwfn program package at the B3LYP/SDD, 6-31g\* level of theory. Dashed red lines indicate areas of charge concentration ( $\nabla^2\rho(r) < 0$ ) while

dotted black lines show areas of charge depletion ( $\nabla^2\rho(r)>0$ ). Black dots indicate BCPs. Solid brown lines connecting the atomic nuclei are the bond paths. Blue, and orange dots indicate BCPs and RCPs.

**Fig.3** Molecular structure and labeling diagram of **4** ((a) and (b) two different view of **4**). Selected bond lengths (Å) and bond angles (°): W1-W2 2.848, B2-B3 1.63(4), B4-B3 1.76(4), B5-B4 1.85(4), W1-B5 2.30(4), W2-B4 2.32(3), W1-Te1 2.748(2); W1-Te1-W2 63.37(5), B3-B2-W2 106.1(13), B1-B2-B4 98.0(18), W1-B5-W2 76.4(12).

**Fig.4** Sequence of diamond-square-diamond (DSD) process converting the heptagonal bipyramid into the *oblatoarachno* deltahedron **4**.

**Fig. 5** (a) showing 3c-2e bonding orbital of B1-B2-B3 from NBO analysis of **4'** (contour value:  $\pm 0.05$  [e/bohr<sup>3</sup>]<sup>1/2</sup>), (b) showing the contour line diagrams of the Laplacian of the electron density,  $\nabla^2\rho(r)$  of B1-B2-B3 plane in **4'** that generated using the Multiwfn program package at the B3LYP/SDD, 6-31g\* level of theory. Dashed red lines indicate areas of charge concentration ( $\nabla^2\rho(r)<0$ ) while dotted black lines show areas of charge depletion ( $\nabla^2\rho(r)>0$ ). Black dots indicate BCPs. Solid brown lines connecting the atomic nuclei are the bond paths. Blue, and orange dots indicate BCPs and RCPs.

**Table 2.** Crystallographic data and structure refinement information for compounds **1** and **4**

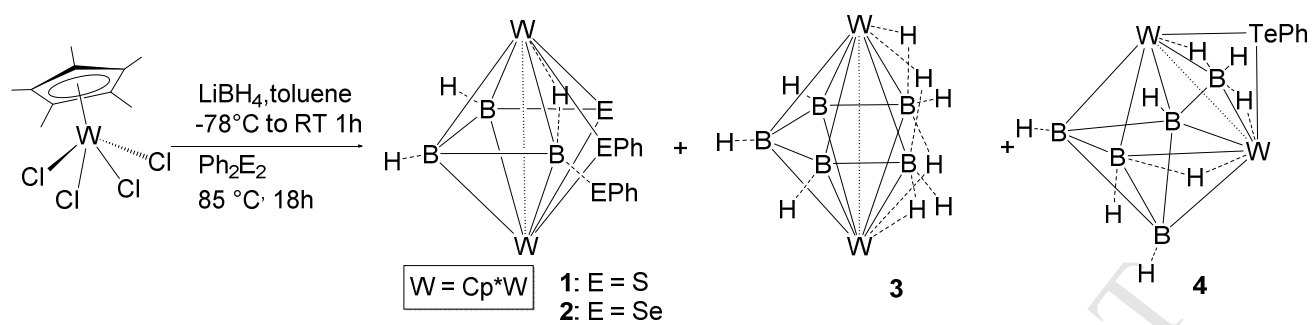


Fig. 1

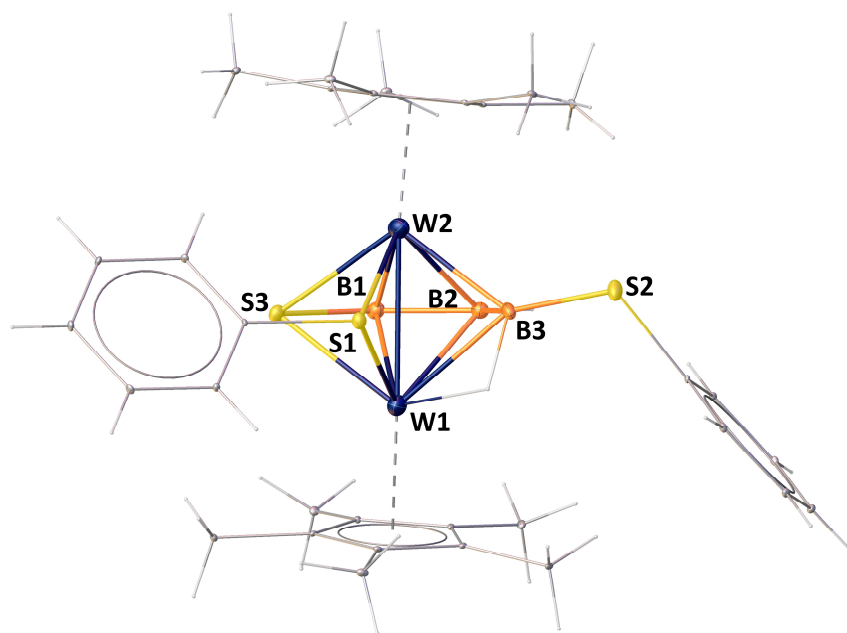


Table 1

Sl No	Compounds	sep	d[M-M] [Å]	d[B-B] <sup>a</sup> [Å]	<sup>11</sup> B NMR	Ref.
1	[(Cp*Ta) <sub>2</sub> B <sub>4</sub> H <sub>10</sub> ]	5	2.89	1.93	0.3, 16.6	23a
2	[(Cp*Cr) <sub>2</sub> B <sub>4</sub> H <sub>8</sub> ]	5	2.87	1.75	34.3, 126.5	22
3	[(Cp*ReH <sub>2</sub> ) <sub>2</sub> B <sub>4</sub> H <sub>4</sub> ]	6	2.81	1.94	1.30, 68.7	20
4	[(Cp*MoCO) <sub>2</sub> B <sub>4</sub> H <sub>6</sub> ]	6	2.92	1.61	63.7, 15.8	16
5	[(Cp*WCO) <sub>2</sub> B <sub>4</sub> H <sub>6</sub> ]	6	--	--	60.4, 7.6	16
6	[(Cp*Mo) <sub>2</sub> B <sub>2</sub> H <sub>5</sub> (BER) <sub>2</sub> (μ-η <sup>1</sup> -ER)] <sup>b</sup>	6	2.69	1.63	84.4, 49.8, 30.4	7a
7	[(Cp*Mo) <sub>2</sub> B <sub>2</sub> H <sub>5</sub> (BER) <sub>2</sub> (μ-η <sup>1</sup> -ER)] <sup>c</sup>	6	2.71	1.65	78.8, 54.0, 19.2	7a
8	[(Cp*Mo) <sub>2</sub> B <sub>2</sub> S <sub>2</sub> H <sub>2</sub> (μ-η <sup>1</sup> -S)]	6	2.63	1.69	18.8	7a
9	[(Cp*W) <sub>2</sub> (μ-S)(μ-η <sup>4</sup> :η <sup>4</sup> -S <sub>2</sub> B <sub>2</sub> H <sub>2</sub> )]	6	2.65	1.66	3.52	18c
10	<b>1</b>	6	2.69	1.69	91.8, 73.3, -12.2	*
11	<b>2</b>	6	--	--	108.3, 77.2, 1.3	*
12	[(Cp*Co) <sub>2</sub> B <sub>2</sub> S <sub>2</sub> H <sub>2</sub> ]	8	3.07	1.73	22.7	25b
13	[(Cp*Rh) <sub>2</sub> B <sub>2</sub> Se <sub>2</sub> H <sub>2</sub> ]	8	3.42	1.74	23.9	24
14	[(Cp*Ir) <sub>2</sub> B <sub>2</sub> Se <sub>2</sub> H <sub>2</sub> ]	8	3.46	1.75	7.3	24

<sup>a</sup>Distance between two boron atoms (B1 and B2) in the M<sub>2</sub>B<sub>2</sub> tetrahedron core of bicapped tetrahedral geometry. <sup>b</sup>E = S, R = 2,6-(<sup>t</sup>Bu)<sub>2</sub>C<sub>6</sub>H<sub>2</sub>OH. <sup>c</sup>E = Se, R = Ph. \*This work

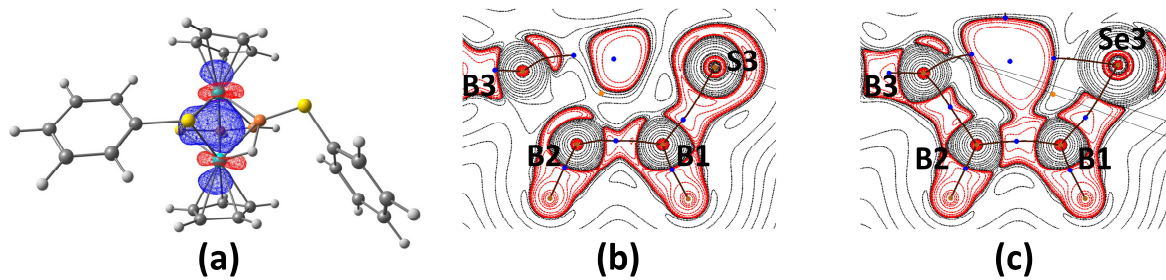


Fig.3

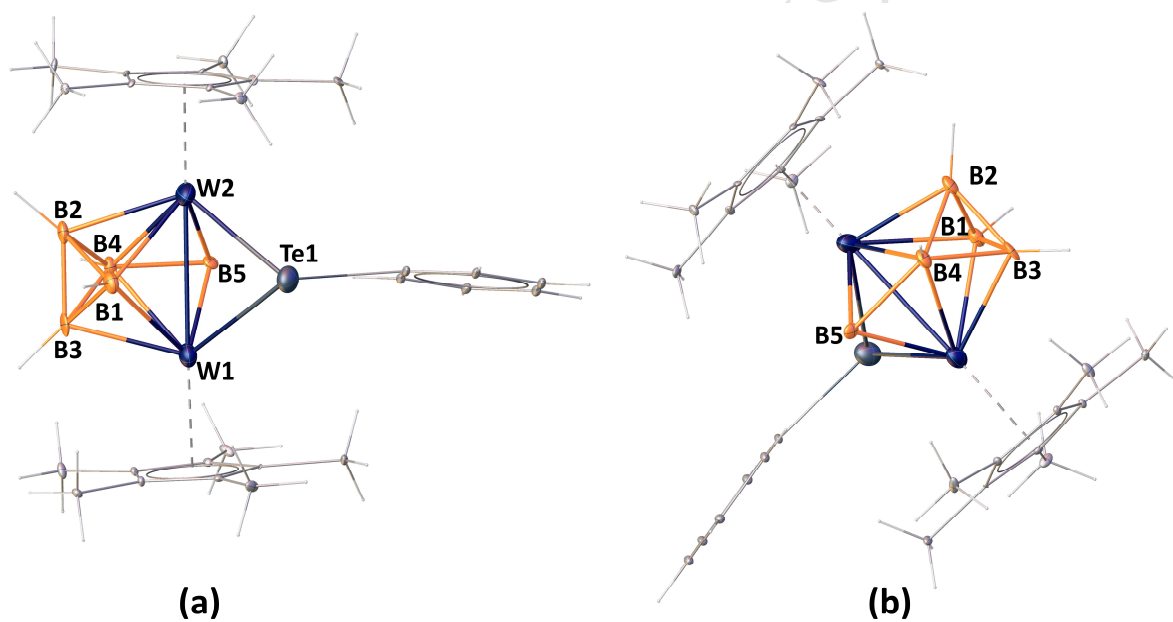
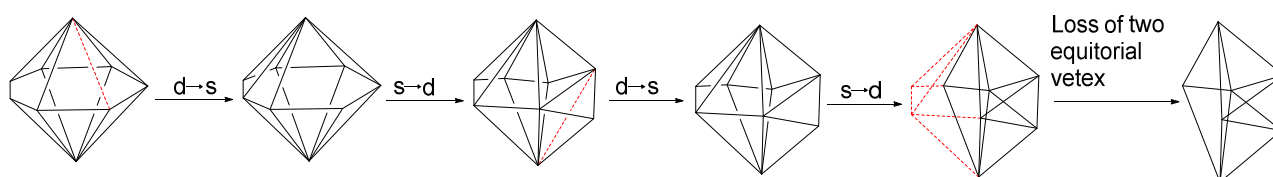


Fig.4



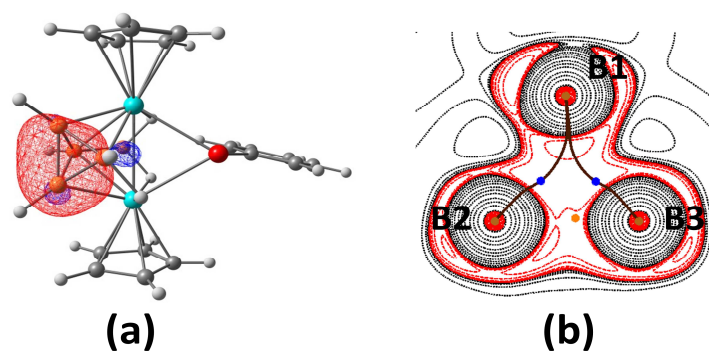


Table 2

	1	4
empirical formula	$C_{32}H_{43}B_3S_3W_2$	$C_{26}H_{39}B_5TeW_2$
CCDC NO	1878746	1878747
formula weight	923.97	900.92
crystal system	Orthorombic	triclinic
space group	$F 2 -2d$	$P -1$
$a$ (Å)	18.003(2)	11.202(2)
$b$ (Å)	46.906(5)	14.438(3)
$c$ (Å)	15.5706(17)	18.750(4)
$\alpha$ (°)	90	88.407(5)
$\beta$ (°)	90	81.888(4)
$\gamma$ (°)	90	80.168(5)
$V$ (Å <sup>3</sup> )	13149(2)	2958.1(11)
$Z$	16	4
$D_{calc}$ (g/cm <sup>3</sup> )	1.867	2.023
$F$ (000)	7136	1680
$\mu$ (mm <sup>-1</sup> )	7.205	8.751
$\theta$ Range (°)	1.737-28.32	1.05-28.5
no. of total refins collected	53195	55441
no. of unique refins [ $I > 2\sigma(I)$ ]	7201	55441

max and min transmission	0.411 and 0.327	0.354 and 0.274
goodness-of-fit on $F^2$	1.010	1.081
final $R$ indices [ $I > 2\sigma(I)$ ]	$R1 = 0.0231$ $wR2 = 0.0337$	$R1 = 0.0846$ $wR2 = 0.2557$
$R$ indices (all data)	$R1 = 0.0271$ $wR2 = 0.0345$	$R1 = 0.1032$ $wR2 = 0.2694$

---

**Research Highlights:**

- Explored the synthesis of tungstaheteroboranes employing diphenyl dichalcogenides.
- Formation of  $[(Cp^*W)_2(\mu-EPh)(\mu_3-E)(\mu-H)(B_3H_2EPh)]$  (E= S and Se) supports the existence of saturated tungstaborane compound  $[(Cp^*W)_2B_4H_{10}]$  as the intermediate.
- $[(Cp^*W)_2(\mu-TePh)B_5H_5(\mu-H)_3]$ , with capped octahedron geometry is exceptional due to the presence of three W-H-B bridging hydrogens.